Food Chemistry: Molecular Sciences 5 (2022) 100135

Contents lists available at ScienceDirect

Food Chemistry: Molecular Sciences

journal homepage: www.sciencedirect.com/journal/food-chemistry-molecular-sciences

Fe^{2+} protects postharvest pitaya (*Hylocereus undulatus britt)* from *Aspergillus. flavus* infection by directly binding its genomic DNA

Lishan Yao, Tao Zhang, Shurui Peng, Dan Xu, Zhenbin Liu, Hongbo Li, Liangbin Hu *, Haizhen Mo *

School of Food and Biological Engineering, Shaanxi University of Science and Technology, Xi'an 710021, China

ARTICLE INFO

Keywords:
Pitaya
A. flavus
Fe^{2+}
Antifungal agent
Mechanism

ABSTRACT

Aspergillus flavus (A. flavus) is a postharvest fungus, causing pitaya fruit decay and limiting pitaya value and shelf life. However, safer and more efficient methods for preventing *A. flavus* contamination for pitaya fruit remain to be investigated. In this study, we successfully proved exogenous Fe^{2+} could inhibit *A. flavus* colonization in pitaya fruit and extend pitaya's shelf life after harvest. Moreover, gel electrophoresis, CD analysis and Raman spectrum tests revealed Fe^{2+} could more effectively and thoroughly promote conidial death by directly binding to *A. flavus* DNA. Increased expression of DNA damage repair-related genes after Fe^{2+} treatment was observed by transcription analysis, which might eventually lead to SOS response in *A. flavus*. These results indicated Fe^{2+} could prevent *A. flavus* infestation on pitaya in a novel, quickly responsive mechanism. Our results shed light on the potential application of Fe^{2+} in the food industry and provided a more universal antifungal agent against food pathogens.

1. Introduction

Pitaya (*Hylocereus undulatus britt*) has become one of the most popular trends in the fruit consumption market, owing to its desirable taste and rich sources of health-promoting antioxidant compounds (Ong, Wen, Mohamad, Sieo, & Tey, 2014). Nevertheless, the quality of pitaya is often challenged by postharvest fungal disease. It has been reported that more than 40 % of postharvest fruit and vegetables are lost, which is largely due to decay caused by fungal attack. Among these, *Aspergillus flavus* (*A. flavus*) is believed to be the main contributor to pitaya fungal contamination, which results in pitaya deterioration and rapid senescence and inevitably leads to physiological responses, including shrinkage, softening, weight loss, decay of the fruit and changes in flavor and antifungal-related matter. (Zahid, Ali, Siddiqui, & Maqbool, 2013; Toivonen & Brummell David, 2008). Apart from the ill effect of *A. flavus* on fruit quality, the secondary metabolite aflatoxin B_1 (AFB_1) it produced has been put into Group 1 carcinogen by IARC (the International Agency for Research on Cancer), and the toxin can be transferred to humans and animals through contaminated foods, provoking life-threatening diseases to humans, such as acute poisonings, immune-system dysfunctions, and stunted growth in children. High-dose intake of AFB_1 even leads to death (Fiore et al., 2018; Umesha et al., 2017). With global warming, the infection of pitaya with fungal diseases, especially *A. flavus*, has increased, thus limiting its development and marketing potential.

For the past few decades, the control of fungi in pitaya has mainly been achieved by application of synthetic fungicides (Jiang, Chen, Lee, & Chang, 2020; Pace & Cefola, 2021). However, the successive and extensive use of these fungicides not only causes drug resistance but also raises concerns about the toxicity of chemical fungicides to both humans and the environment. Therefore, safer and more environmentally friendly strategies to protect pitaya from fungal infection are urgently needed. Fe^{2+}, as an essential chemical element, is a bio efficient and inexpensive iron nutrient fortifier and is often used as an iron supplement for children and pregnant women (Harvey, Zkik, Auges, & Clavel, 2016). It is one of the most important metallic elements in life, participates in many biological processes and is considered as a better antimicrobial agent since it can be degraded by human body and does not cause toxicity. (Jomova & Valko, 2011). Newly studies have suggested that Fe^{2+} facilitated ferroptosis in *Magnaporthe oryzae*, eventually affected the growth of hyphae and reduced infection ability of fungi (Shen, Liang, Yang, Deng, & Naqvi, 2020). Our previous study proved that exogenous 0.5 mM Fe^{2+} induced ferroptosis in *A. flavus* spores and suppressed growth of *A. flavus* (Yao, Ban, Peng, Xu, Li, & Mo, 2021).

* Corresponding authors.
E-mail addresses: hulb@sust.edu.cn (L. Hu), mohz@sust.edu.cn (H. Mo).

https://doi.org/10.1016/j.fochms.2022.100135
Received 6 July 2022; Received in revised form 30 August 2022; Accepted 17 September 2022
Available online 21 September 2022

A. flavus is one of the most important fungi causing pitaya decay after harvest; however, few studies have focused on the antifungal effects of Fe^{2+} on food preservation. To test the effect of Fe^{2+} on preservation and sterilization of pitaya, $FeSO_4$ was used to treat postharvest pitaya fruit. The conidial mass, weight loss ratio, fruit decay rate, total soluble solids, titratable acidity, soluble sugars, total betalain content, phenols, flavonoids, malondialdehydehyde content and antioxidant-related enzyme activity (*CAT, SOD, POD*) were measured, and the possible physiological mechanism was explored in our study. The results will provide a theoretical basis for scientific storage and raise the potential application of Fe^{2+} as a safer, less expensive and more eco-friendly antifungal agent for food storage.

2. Materials and methods

2.1. Chemicals and strains

A. flavus NRRL3357 was obtained from Sun Yat-sen University (Guangdong, China) and cultivated on potato dextrose agar (PDA) medium (Becton, Dickinson and Company, USA) at 30 °C. The spore suspension was harvested with 0.05 % Triton X-100, and the spore number was counted using a hemocytometer under a microscope. DNA was extracted using a Biospin fungus genomic DNA extraction kit from cultured *A. flavus* hyphae, and a Nanodrop (Nanodrop ND-1000 UV, Thermo Scientific) was used to measure the purity of DNA using an absorption ratio of 260 to A280, the DNA concentration was measured by Nanodrop and adjusted to a final concentration of 2×10^3 ng/μL. Ferrous sulfate heptahydrate ($FeSO_4{\cdot}7H_2O$) was purchased from Sigma. Chemical kits used for testing activity of *CAT* (BC0200-50 T/48S), *POD* (BC0090-50 T/48S) and *SOD* (BC0170-50 T/24S) were purchased from Solarbio (Beijing Solarbio Science & Technology Co., ltd.). All other chemical agents were analytical grade.

2.2. Spore viability measurement

Spore viability assay was performed to evaluate the inhibitory effect of Fe^{2+} on spore according to our previous methods (Yao et al., 2021). Briefly, in spot dilution assay, 5 μL of serial-diluted *A. flavus* spore suspension (10^7, 10^6, 10^5, 10^4, 10^3 CFU/mL) were dropped onto each of Sabouraud solid plate with preadded Fe^{2+} to the final concentration of 0, 0.25, 0.5, 1, 2, 3 mM, respectively, and these plates were subjected to a stationary culture for 3 days at 30 °C.

2.3. Plant materials and treatments

White pitaya fruit with similar weight, size, color, maturity and no obvious external mechanical damage were purchased at local market and picked for preservation and sterilization experiments. A total of 10^5 CFU/mL *A. flavus* spores were used for the infection test, and 3 mM Fe^{2+} was prepared. A total of 48 fruit were selected, after disinfecting the surface of the fruit, one group (at least 12) fruit were soaked in the solution of Fe^{2+} for 10 min, dried naturally, repeated the treatment three times, one group fruit with only disinfecting the surface as control; in the sterilization test, fruit were soaked in A *flavus* spore suspension for 10 min, then soaked again after natural air drying, repeated three times, then divided into two groups, one as control, the other was soaked in 10 mL Fe^{2+} solution for 10 min, dried naturally, repeated three times. All fruit were sampled, observed and measured after 7 d cultured in a 25℃ incubator. The pulp on the equatorial line was cut and quickly frozen in a −80℃ refrigerator with liquid nitrogen for index measurement. Each index was measured three times, and the average value was taken.

2.3.1. Conidial mass assay

The spores on the pitaya surface were removed and soaked with phosphate-buffered saline (PBS, pH 7.4) and then stained with 1 μg/mL SYTO™ 9 Green Fluorescent (Beyotime Institute of Biotechnology, China) at 4 °C for 30 min in the dark, followed by observation under a flow cytometer (Beckman CytoFLEX FCM).

2.3.2. Weight loss ratio (WLR)

The pitaya fruit before and after the test was weighed, and the weight loss ratio was calculated according to the following formula:

$$\mathrm{WLR}(\%) = \mathrm{Weight(before\ test)} - \mathrm{Weight(after\ test)}/\mathrm{Weight(before\ test)} \times 100$$

2.3.3. Fruit decay rate (FRI) and firmness

The decay severity for each fruit was divided into five grades according to the percentage of decay area in the whole fruit: 1 = 0–1 %, 2 = 2 %-25 %, 3 = 25 %-50 %, 4 = 50 %-75 %, and 5 = 75 %-100 %. This grade was then converted into the fruit decay rate (FRI) as follows:

$$\mathrm{FRI}\ (\%) = \Sigma(\mathrm{grade} \times \mathrm{number\ of\ fruit\ in\ the\ grade})/(5 \times \mathrm{total\ number\ of\ fruit}) \times 100$$

The firmness of pitaya fruit was measured at three equatorial points of the peeled fruit using a handheld fruit hardness tester (GY-3, Shanghai Grows Precision Instrument Co., ltd., Shanghai, China) with two probes (diameters: 8 and 11 mm) and expressed as N.

2.3.4. Total soluble solid (TSS), titratable acidity (TA) and soluble sugar content (SSC)

The total soluble solids were measured by a portable refractometer. Briefly, pitaya juices were dropped on the clean prism surface of the refractometer, and the refractometer was faced to the light. The scale shown in the refractometer is the total soluble solid of the fruit. The titratable acidity (TA) was determined using extracted pitaya juices by volumetric titration with NaOH, TA in the juice was a percentage of malic acid as the dominant organic acid in the fruit. The total soluble sugar content was measured through the anthrone-sulfuric acid colorimetric method using a spectrophotometer (HIRP V1700G, Hirp International Trade Co., ltd., Shanghai, China) at 620 nm and calculated with a glucose standard curve and is expressed as g/L.

2.3.5. Malondialdehyde (MDA) content and total betalain, phenol and flavonoid contents

The MDA content was determined by thiobarbituric acid method. One gram of fresh pitaya fruit was ground into a homogenate in 5.0 mL of 10 % TCA (trichloroacetic acid) and centrifuged at 10,000 × g for 20 min at 4 °C. Then, 2.0 mL of supernatant was taken, 2.0 mL of 0.67 % TBA (thiobarbituric acid) was added, and the supernatant was boiled for 20 min. After cooling, the supernatant was centrifuged again, and the absorbance values were measured at 450 nm, 532 nm and 600 nm.

Under high temperature and acidic conditions, MDA can react with TBA to form a reddish-brown trimethyl complex (3,5,5-trimethyloxazole-2,4-dione), which has a maximum absorbance value at 532 nm. However, soluble carbohydrates in fruit tissues can interact with MDA-TBA products and have absorbance values at 532 and 450 nm. To eliminate this interference, the following empirical formula was used to eliminate the soluble carbohydrate interference:

$$C\ (\mu mol/L) = 6.45 \times (OD532 - OD600) - 0.56 \times OD450$$

Based on the calculated MDA concentration in the supernatant, the MDA in the whole fresh pitaya was attained as follows:

$$CMDA\ (mol/Kg) = C \times V/Vs \times W \times 1000000$$

The flesh of pitaya (2 g) was soaked with 20 mL of methanol (80 %, v/v) and sonicated for 10 min in a bath (KQ5200DE, Prevnext). The methanolic extract was stirred for 20 min at room temperature and centrifuged at 5,000 × g for 10 min (Thermo Scientific, Legend Micro17, Waltham, MA, USA). One milliliter of supernatant was collected and fourfold diluted, and the concentrations of betalain were determined by

spectrophotometry at 538 nm wavelength. The total content of betalain was expressed as g per kg of fresh pitaya weight:

$$B(g/kg) = A538 \times W \times V \times Df/(\varepsilon \times l \times m) \times 1000$$

where B is the content of betalain, A538 is the absorbance at 538 nm, W is the molecular weight (550 g·mol^{-1}), V is the volume of the extracted solution (mL), D*f* is the dilution factor, ε is the molar extinction coefficient (65,000 L·mol^{-1}··cm^{-1}), m is the mass of the sample (2 g), and *l* is the length of the cell (1 cm).

According to Folin-Ciocalteu's procedure, the content of total phenols was determined from the reaction of 1 mL of the methanolic extracts and 2.5 mL of 1:1 (v/v) diluted Folin-Ciocalteu's reagent. Then, 2 mL of 7.5 % (w/v) Na_2CO_3 solution was added and incubated for 5 min at 50 °C, and the absorbance was measured at 760 nm. A standard curve of gallic acid was made to estimate phenol content, and the results were expressed as g/kg.

Flavonoid content was assessed as followed: First, 3.7 mL of the methanolic extracts, 0.15 mL of 10 % $AlCl_3{\cdot}6H_2O$ and 0.15 mL of 5 % $NaNO_2$ were mixed. After 5 min, 1 mL of 1 M NaOH was added prior to the measurement at 510 nm. The concentration of flavonoids was estimated from the calibration curve using rutin as the standard and expressed as (g/kg).

2.3.6. Assessment of superoxide dismutase (SOD), peroxidase (POD), and catalase (CAT) activities

The activities of *SOD, POD* and *CAT* were measured using a biochemical kit (Beijing Solarbio Science & Technology Co., ltd.) following the manufacturer's guidelines. Briefly, *SOD* is widely present in animals, plants, microorganisms and cultured cells, and catalyzes the disorganization of superoxide anions ($O_2\bullet^-$), $O_2\bullet^-$ can reduce nitro-blue tetrazolium to generate formazan, which is absorbed at 560 nm; *SOD* activity can be reflected by absorption at 560 nm through inhibiting the formation of formazan; *POD* has the dual effect of eliminating H_2O_2 and toxicity of phenolic and amine, *POD* catalyzes specific substrates with characteristic absorption at 470 nm; *CAT* is the most important H_2O_2 scavenging enzyme and plays an important role in reactive oxygen species scavenging systems, H_2O_2 has a characteristic absorption peak at 240 nm, which decreases when *CAT* decomposed H_2O_2, so that *CAT* activity can be calculated according to the change of absorbance. The activity of these enzymes was expressed as units (U) kg^{-1}.

2.4. Genomic DNA break detection

The *A. flavus* suspension (10^5 CFU/mL) exposed to 2 mM Fe^{2+} for 20 min and 1 h were stained with TUNEL (10 μg/mL) for 30 min at 4 °C. The broken genomic DNA was observed with a flow cytometer (FCM, Beckman CytoFLEX).

2.5. RNA-seq analysis of A. Flavus spores after Fe^{2+} treatment

A 10^6 CFU/mL spore suspension exposed to 2 mM Fe^{2+} for 20 min and 1 h was sampled and ground in liquid nitrogen. Total RNA was extracted using a total RNA extractor (TRIzol) kit (Yili, Shanghai, China). The integrity and quality of RNA were evaluated using a 1 % agarose gel and an Agilent Technologies 2100 Bioanalyzer. High-quality RNA samples were prepared for cDNA library construction and sequencing. FastQC software was used for data quality evaluation, and sequenced clean reads were obtained by filtering out low-quality reads and adaptor contamination, then mapped against predicted transcripts of the *A. flavus* NRRL 3357 genome. The differentially expressed genes (DEGs) were filtered by p value < 0.05. DEGs related to DNA repair between the control and treatments were selected at significant levels calculated by Fisher, and DEGs were visualized by a heatmap. All data are the average of three replications.

2.6. Gel electrophoresis

A gel electrophoresis system was used to test Fe^{2+} damage on purified genomic DNA, amplified PCR products and process of PCR. A 10 μL interaction system was set containing 2 μL of Fe^{2+} solution, which was adjusted to final concentrations of 1 mM, 2 mM, 3 mM and 8 μL of DNA or PCR products. Then, 1 μL of 10 × DNA loading buffer was added to the system after 30 min treatment, and 1 % gel was prepared for electrophoresis. The system was under electrophoresis for 30 min at 120 V and 400 mA, and then the image was observed under a UV lamp. To test the effects of Fe^{2+} on the process of PCR, Fe^{2+} solution was added to the PCR system at final concentrations of 1 mM, 2 mM, and 3 mM. A 20 μL PCR system used was shown in Table S1, the procedure was as shown in Table S2, and the product was measured using gel electrophoresis as mentioned above.

2.7. Circular dichroism (CD) experiments

CD spectral analysis were determined on Chirascan Plus equipment (V-100, Applied Photophysics, UK). Briefly, DNA samples were prepared and mixed with Fe^{2+} saline solution for 30 min, and the solution was adjusted to pH 7.3. The temperature was controlled by water circulation. The CD spectra were collected between 200 and 500 nm with the bandwidth at a 1 nm interval using a JASCO-720CD spectropolarimeter. All spectral data were the average of three technical duplicates and three biological duplicates.

2.8. Confocal Raman microspectrometer

Well-prepared *A. flavus* DNA solution was used in our test and Fe^{2+} was added to DNA solutions to achieve a final concentration of 2 mM, then the liquids were placed on specific liquid-used glass plates. A Renishaw (Gloucestershire, UK) inVia confocal Raman spectrometer coupled to a DMLM Leica microscope was used for the measurement. A 785 nm laser source, 600 notched grating, 50X long focal length was adopted, and the laser power was 30 mW. Raman spectra in the range of 800–2000 cm^{-1} were collected using a 50 (NA = 0.5) focal length lens and 10.5 mm working distance, the spectra were acquired at 30 min afterward. The integration time was 8 s, and the integration was performed in triplicate. All solutions were maintained at room temperature during the experiment.

2.9. Statistical analysis

IBM SPSS Statistics v20 Software was used for statistical analysis and quantitative detection data in each result is presented as the mean ± standard deviation (SD) of at least three replicated measurements. A t test was used to analyze the significant differences between two groups, multiple groups' comparison was achieved by one way ANOVA analysis and Duncan. Statistically significant difference was considered at p value < 0.05. All charts were accomplished using OriginPro 2021.

3. Results and discussion

3.1. Exogenous 3 mM Fe^{2+} completely inhibited A. favus spore germination

In order to evaluate the influence of exogenous Fe^{2+} on *A. flavus* growth and germination, different concentrations of Fe^{2+} were applied to *A. flavus* spore suspension. As shown by spot dilution assay, the antifungal activity of Fe^{2+} was observed in a dose dependent manner, exogenous 3 mM Fe^{2+} could completely inhibited *A. flavus* germination (Fig. 1), which was consistent with our previous study (Yao et al., 2021). Therefore, 3 mM Fe^{2+} was selected in our following test to explore the effect of Fe^{2+} on pitaya preservation and sterilization experiments.

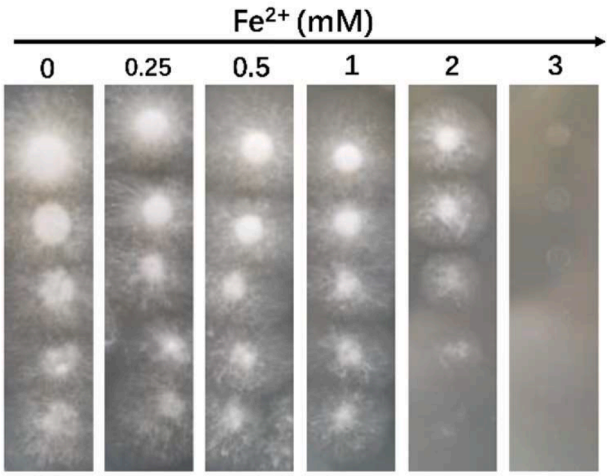

Fig. 1. Inhibitory effects of Fe^{2+} on the spore growth of *A. flavus* NRRL3357.

3.2. Exogenous Fe^{2+} extended pitaya shelf life and inhibited fungal infestation

To test the potential effects of Fe^{2+} on extending shelf life and preventing pathogenic colonization of pitaya fruit, 3 mM Fe^{2+} was applied for preservation and sterilization tests (Fig. 2). As shown in Fig. 2, Fe^{2+} obviously alleviated the decay phenotypes after long time storage and reduced contamination caused by *A. flavus*.

Water and organic matter in the fruit can be consumed by respiratory metabolism and pathogen colonies, resulting in weight loss, reduced firmness and decay on the surface of the fruit. As shown in Fig. 3**A**, the application of Fe^{2+} alleviated the total conidial mass after *A. flavus* contamination, and weight loss rate (WLR) and fruit decay rate (FRI) were suppressed by 34.07 % and 49.98 %, respectively, in Fe^{2+}-treated pitaya fruit compared to untreated fruit. Fe^{2+} also retained fruit weight and constrained fruit decay after *A. flavus* infection, which suppressed weight loss and fruit rot by 7.87 % and 40 %, respectively (Fig. 3**B-C**).

Fe^{2+} could retain pitaya firmness after *A. flavus* treatment and maintain flavor in pitaya under *A. flavus* treatment, where Fe^{2+} markedly retained TA content. Decreased TA in fresh pitaya fruit could be attributed to accelerated respiratory intensity, which caused consumption of carbohydrates and organic acids. In our study, Fe^{2+} suppressed the decline in TA during storage, indicating that Fe^{2+} probably acted as an inhibitor, affecting the respiratory mode in pitaya fruit. However, no statistically significant difference was observed in total soluble solids (TSS) and soluble sugar content (SSC) after Fe^{2+} treatment in either the preservation or sterilization test. It indicated that exogenous Fe^{2+} treatment could not affect the ripening degree of pitaya after harvest, for total soluble solids (TSS) and soluble sugar content (SSC) were believed to be an indicator of fruit ripening. (Fig. 4**A-D**).

3.3. Effects of Fe^{2+} on MDA, total betalain, phenol and flavonoid contents

Malondialdehyde (MDA), as an indicator of cell membrane oxidation, is greatly induced during pitaya storage due to fruit senescence and pathogen attack. MDA content was measured based on Fe^{2+} treatment during preservation and *A. flavus* contamination. The result showed that MDA content remained unchanged after Fe^{2+} treatment during preservation. Considerable decreased MDA was detected after Fe^{2+} exposure under *A. flavus* treatment (Fig. 4**E**). These results suggested that increased MDA content might prior be attributed to pathogen invasion, and Fe^{2+} could protect cell membranes from oxidative damage, thus reducing MDA content. The result indicated that Fe^{2+} could not only extend pitaya shelf life but also shield cell membrane from oxidation after *A. flavus*. Betalain, as a natural water-soluble polyphenolic pigment, is responsible for its high antioxidant capacity, which is beneficial for human health. Fig. 4**F** showed that Fe^{2+} suppressed the reduction in betalain concentrations during preservation and defense

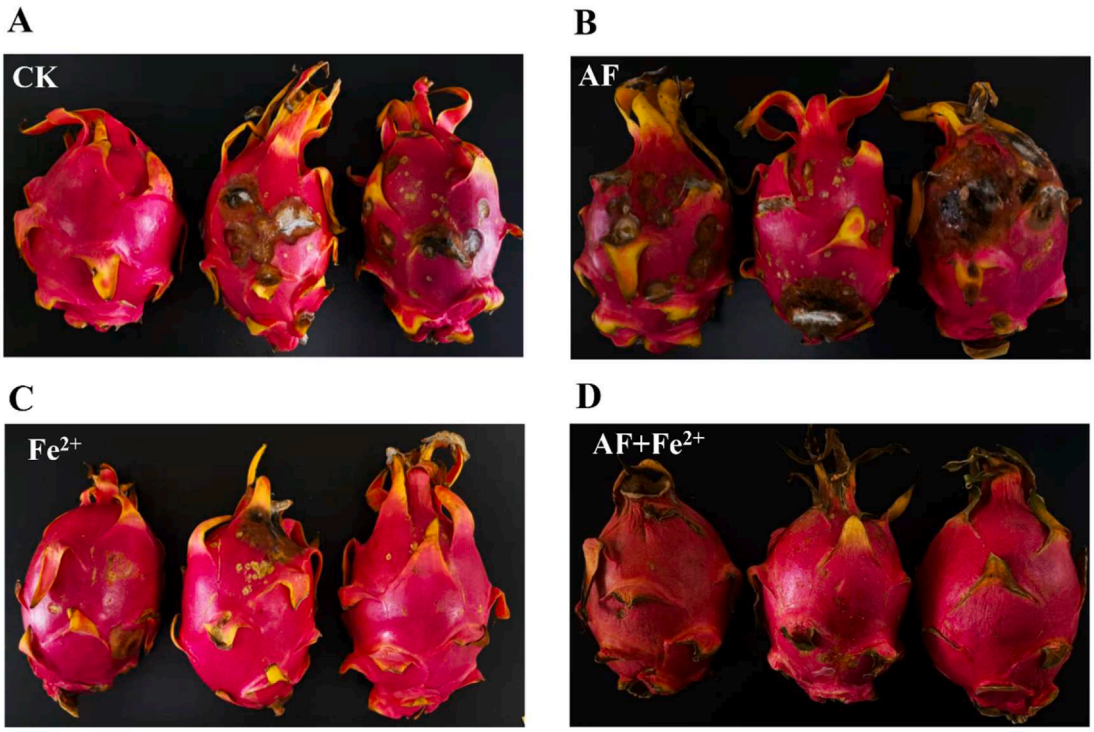

Fig. 2. Phenotypes of Fe^{2+} application in pitaya preservation and A. *flavus* sterilization. Pitaya without any treatment as a control (A); pitaya inoculated with 10^5 CFU/mL A. *flavus* spore suspension (B); pitaya inoculated with Fe^{2+} for the preservation test (C); pitaya inoculated with 10^5 CFU/mL A. *flavus* spore suspension and soaked with Fe^{2+} for the sterilization test (D). All fruit were stored at 25 ℃ for 7 d.

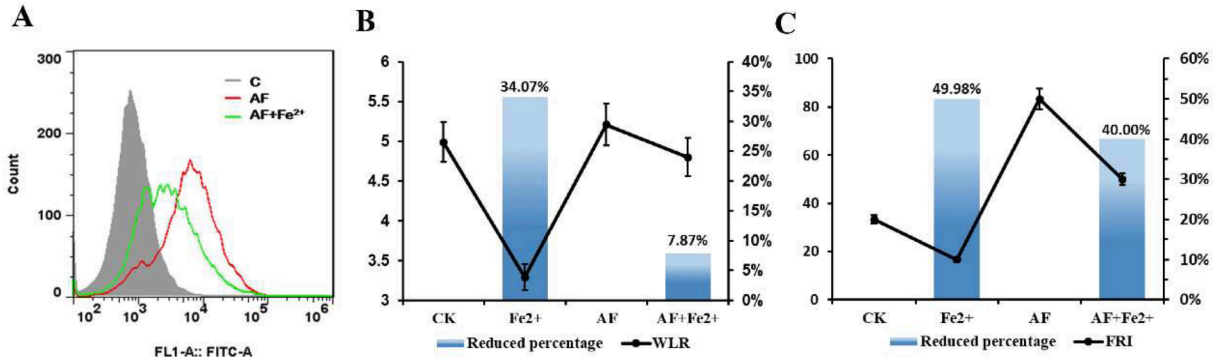

Fig. 3. Conidial mass (A), weight loss rate (WLR) (B) and fruit decay rate (FRI) (C) of pitaya fruit after Fe^{2+} treatment in preservation and sterilization tests.

against *A. flavus*.

3.4. Effects of Fe^{2+} on total phenol, flavonoid, DPPH, SOD, POD, and CAT expression

As the main active antioxidant response, the phenol content was higher after Fe^{2+} treatment than in the control during preservation and *A. flavus* treatment, while the total flavonoid content was unchanged (Fig. 4**G-H**). The expression of DPPH, *SOD, POD* and *CAT* showed a similar gradually elevated trend, and improved activity of these enzymes was detected after *A. flavus* contamination; moreover, Fe^{2+} exposure could significantly induce their expression, except for DPPH, which was decreased during the preservation process (Fig. 4**I-L**). These results revealed that Fe^{2+} could activate antioxidant reaction of pitaya fruit by promoting expression of antioxidant-related enzymes, especially in response to *A. flavus* infection.

Above all, in terms of postharvest preservation and resistance to *A flavus* infestation, Fe^{2+} showed potential capability to extend the shelf life of pitaya fruit and ability to combat colonization of *A. flavus*.

3.5. Fe^{2+} induced DNA damage of A. Flavus

To explore whether Fe^{2+} induced *A. flavus* DNA damage, TUNEL staining of *A. flavus* spores after different concentrations of Fe^{2+} treatment was conducted. The phenomenon of DNA breakage after disposal to Fe^{2+} was observed, and a right shift under a flow cytometer was detected after 1 mM Fe^{2+} treatment, indicating that damage occurred in part of the DNA under Fe^{2+} treatment (Fig. 5**A**).

3.6. Fe^{2+} activated DNA damage repair genes and triggered the SOS response

DNA damage further interferes with cellular replication and transcription, even results in genetic mutations and chromosomal lesions, and severe DNA damage usually eventually leads to the SOS response (Loeb, James, Waltersdorph, & Klebanoff, 1988). To further investigate the possible DNA damage-related genes under Fe^{2+} pressure, RNA sequencing analysis in *A. flavus* spores after Fe^{2+} treatment was performed. The data indicated that a total of 49 genes enriched in the DNA damage repair pathway were detected, with only minor variations in the transcription levels between the three replicates, but Fe^{2+} treatment differed significantly from control (**Fig. S1**), where Fe^{2+} increasingly upregulated DNA damage repair-related genes compared to control, including *RAD* gene, a nucleotide excision repair homologous gene, which was reported to be involved in repair of aflatoxin-induced DNA damage in yeast by removing bulky DNA lesions formed by UV light, environmental mutagens or chemicals (Fig. 5**B-C**) (Guo, Breeden, Zarbl, Preston, & Eaton, 2005). These results suggested that Fe^{2+} may trigger DNA damage repair system under exogenous Fe^{2+} accumulation, which was corresponded to previous studies showing that exogenous stress could upregulate DNA damage-inducible genes (Christmann & Kaina, 2013). We assumed that this might be related to the SOS response, because DNA repair genes are usually activated by the SOS response, and this was a survival strategy for microorganisms to survive challenging pressure (Keseler et al., 2013). However, how Fe^{2+} triggers this reaction requires further investigation.

3.7. Fe^{2+} chelated gDNA and affected the PCR process

DNA, as the material basis of life, is of great importance to all living organisms, and its molecular integrity is also necessary for life activities of living organisms. Any lesion or injury to DNA will affect not only its integrity but also the transcription it participates in. Gel electrophoresis is known as a straightforward and convenient method to detect the integrity of DNA and PCR procedures. Therefore, gel electrophoresis analysis under different concentrations of Fe^{2+} was performed in our study to investigate the effects of Fe^{2+} on DNA and PCR processes. Stripe retention was observed in the Fe^{2+}-treated lane both in the gDNA and in the process of PCR, and the levels of retention increased along with the concentrations of Fe^{2+} (Fig. 5**D-F**). These results indicated that Fe^{2+} could cause damage to gDNA and influence PCR procedure. We suspected that Fe^{2+} could directly interact with DNA and might affect DNA conformation and chelate DNA fragments to form a macromolecular substance that finally stuck in the gel hole (Fig. 5**D-F**). It has been proven in similar reports that exposure to Co and Ni could specifically affect DNA polymerization and the accuracy of replication, repair and transcription processes (Kumar, Mishra, Kaur, & Dutta, 2017).

3.8. Effects of Fe^{2+} on the conformation of DNA

CD spectra are good indicator to investigate DNA conformation, to investigate the effects of Fe^{2+} on DNA conformation, a CD experiment was performed in our study. Fig. 6 showed a strong positive peak in the region at approximately 280 nm of *A. flavus* DNA, but the peak decreased in the Fe^{2+}-pretreated DNA trait. It seemed that Fe^{2+} slightly reduced the compactness of DNA structure. A large negative peak was observed in the region of 200–250 nm, Fe^{2+}-pretreated DNA showed opposite spectra compared to DNA and Fe^{2+} solely in this region, which indicated that DNA conformation might change in the presence of Fe^{2+}. In addition, there was a peak at 400 nm, but no difference was observed in the CD spectra among DNA, Fe^{2+} and their Fe^{2+}-pretreated DNA trait. In conclusion, there was a strong interaction between Fe^{2+} and DNA. Fe^{2+} influenced DNA conformation at 200–250 nm and reduced the density of the CD spectrum of DNA. The changes in DNA structure might further affect the function of DNA binding proteins.

3.9. Raman spectra of Fe-DNA complexes

In addition, Raman spectra were utilized to experimentally interrogate the binding and possible intercalation of Fe^{2+} to DNA. Fig. 6**B**

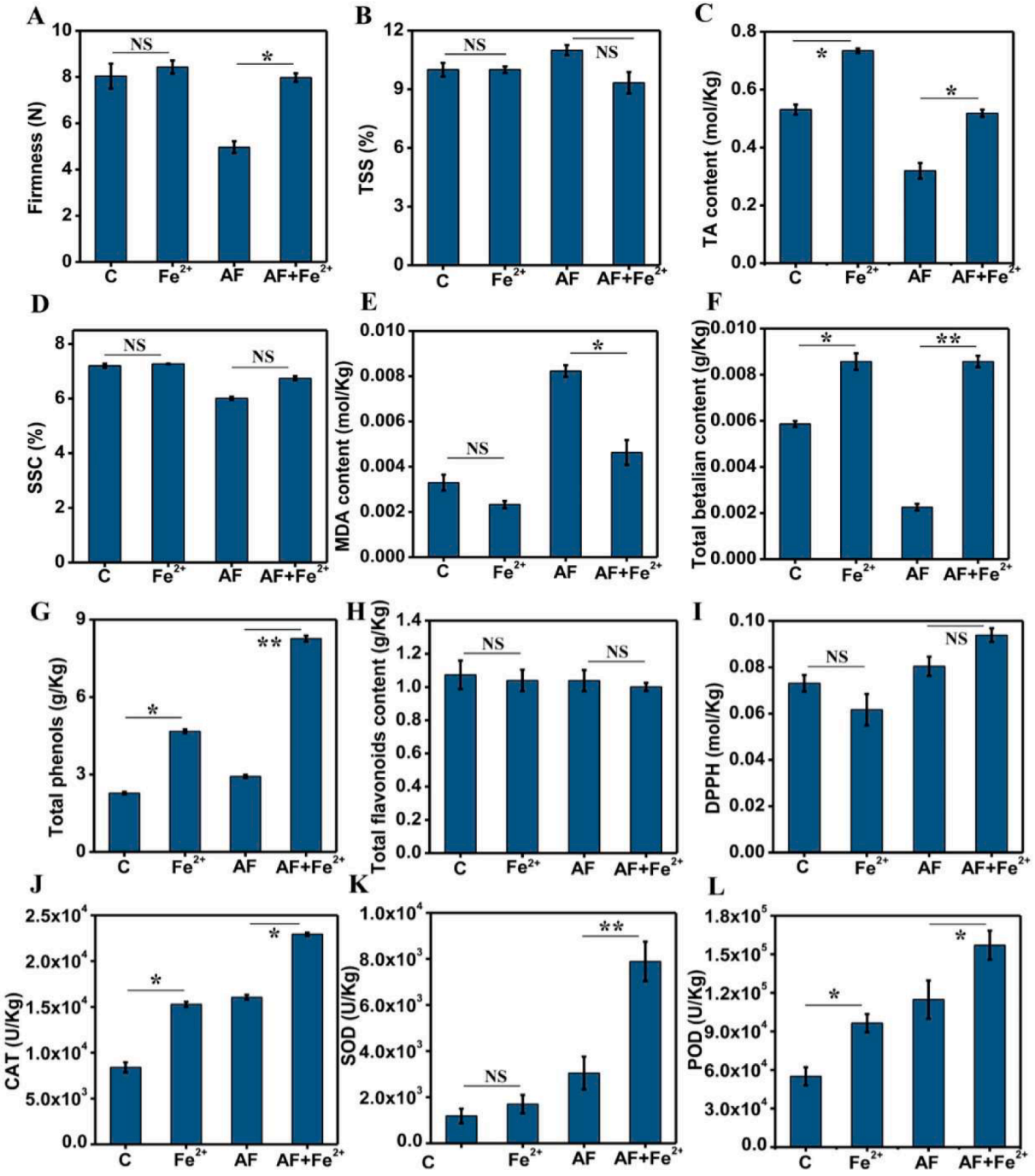

Fig. 4. Firmness (A), total soluble solid (TSS) (B), titratable acidity (TA) (C), soluble sugar content (SSC) (D), malondialdehyde (MDA) content (E), total betalain content (F), total phenol (G), flavonoid (H), antioxidant-related enzyme (DPPH (I), CAT (J), SOD (K) and POD (L)) activities in pitaya fruit after Fe^{2+} treatment in preservation and sterilization tests. NS represents no significant difference between the compared groups; * represents $p < 0.05$, ** represents $p < 0.01$.

indicated a typical spectrum of Fe^{2+} alone at approximately 1400 cm^{-1} and a spectrum of DNA alone at approximately 1370–1390 cm^{-1}, which had been reported to derive from the ring stretching mode of thymine, guanine and adenine bases (Punihaole et al., 2018). When Fe^{2+} premixed with DNA for 30 min, a decrease in the viscosity of solution was observed, and an apparent drop in the spectrum at approximately 1400 cm^{-1} occurred. This result suggested that there was an interaction between Fe^{2+} and DNA. To better highlight the changes, we subtracted the spectrum in Fig. 6C. DNA and Fe^{2+} interaction lowered the significant peak of Fe^{2+} and reduced the peak of DNA, but both Raman shifts of Fe^{2+} and DNA did not change under their interaction. These results might be attributed to the nomadic Fe cation could coordinate with the backbone phosphate group of DNA and change the cleavage ability of DNA, finally resulting in the disappearance of the Raman spectra of Fe^{2+} and DNA. In conclusion, exogenous even low concentration of Fe^{2+} could change the DNA conformation.

4. Discussion

Postharvest decay is the main limiting factor for commercial value and shelf life of pitaya fruit (Xu et al., 2021), which causes 40–50 % loss of postharvest fruit due to pathogen contamination and improper postharvest handling (Bordoh, Ali, Dickinson, Siddiqui, & Romanazzi, 2019). Several approaches, such as cold storage, edible-coating, X-ray,

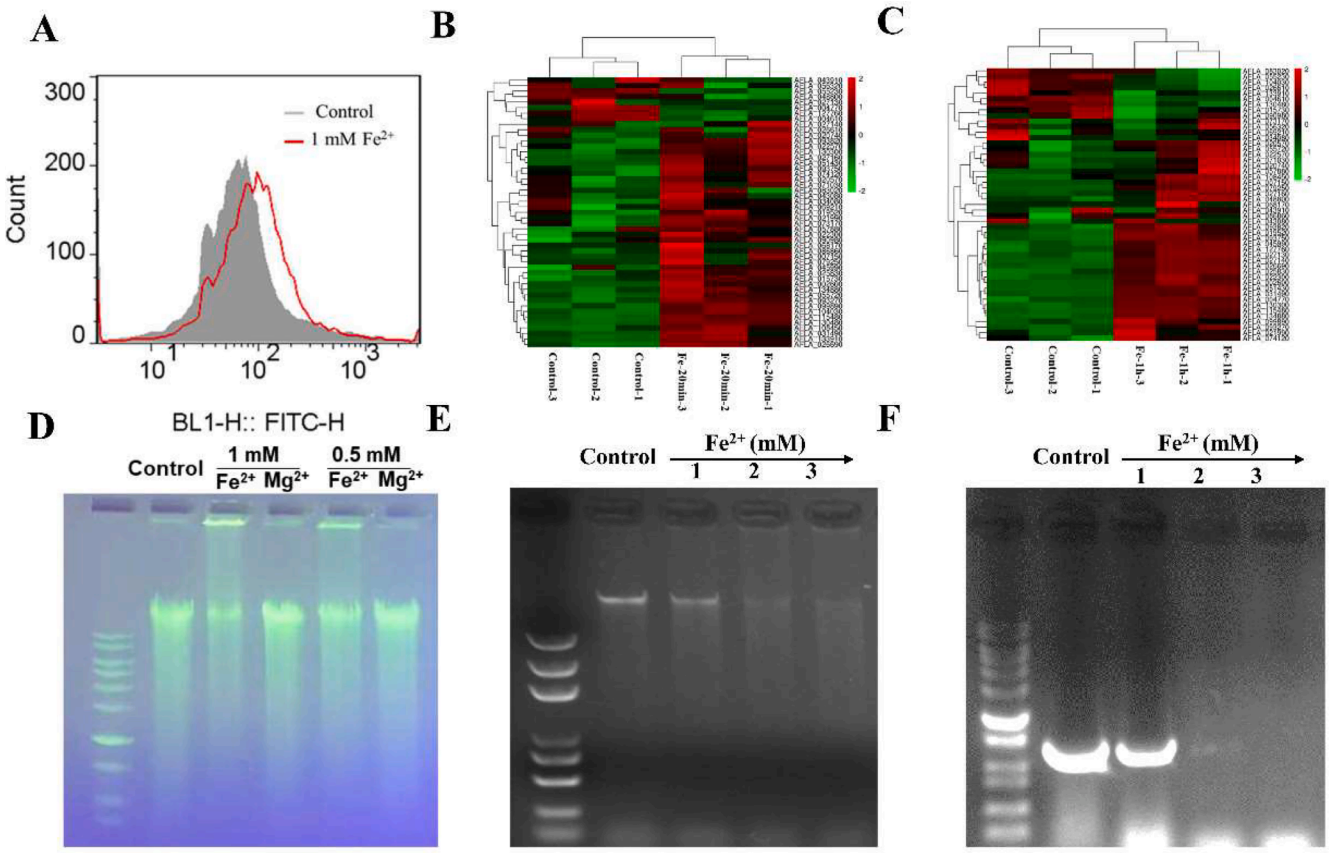

Fig. 5. Exogenous Fe^{2+} induced DNA damage and affected PCR procedure. DNA damage was detected by TUNEL staining and flow cytometry (A); transcriptome analysis of DNA repair-related genes after 20 min (B) of Fe^{2+} treatment and 1 h of treatment (C); Fe^{2+} damage to gDNA of *A. flavus* (D); different concentrations of Fe^{2+} damage to gDNA of *A. flavus* (E); Fe^{2+} damage to the PCR product of *A. flavus* (F). Two microliters of Fe^{2+} solution was added to DNA at final concentrations of 1 mM, 2 mM, and 3 mM, and all DNA solutions were adjusted to the same concentration.

plant hormones, antioxidation additives and antimicrobial agents, have been reported to resist postharvest diseases and hold fruit quality (Ba, Cao, Ning, Chao, & Luo, 2022; Xu et al., 2021). However, these treatments are basic means of delaying fruit senescence and retaining flavor characteristics to various degrees after pathogenic invasion. Despite the additional coating of antibacterial substances, it is still impossible to eliminate pathogens, particularly *A. flavus*. Our study proved that exogenous Fe^{2+} (3 mM) could efficiently suppress weight loss, constrain fruit decay, reduce titratable acid content and retain total betalian content both during the preservation and infection of *A. flavus* (Figs. 1-3). Moreover, Fe^{2+} showed strong potential to suppress malondialdehyde (MDA) content in pitaya fruit after *A. flavus* infection, indicating that Fe^{2+} could not only extend pitaya shelf life but also shield cell membrane from oxidation after *A. flavus* infection **(**Fig. 4**E).**

In addition, Fe^{2+} treatment increased activity of antioxidant-related enzymes, such as *CAT, SOD, and POD,* in pitaya, especially after *A. flavus* attack (Fig. 4**I-L**). It has been reported in some studies that ROS dyshomeostasis during pathogen attack is strongly related to fruit senescence and decay processes (Lin et al., 2017; Xu et al., 2021). ROS dyshomeostasis is the result of an imbalance between ROS production and antioxidant activity. *CAT, SOD* and *POD* are the most studied antioxidant enzymes that act to resist the production of ROS and disintegrate H_2O_2 into H_2O and O_2 (Tan et al., 2020). Enhanced activity of these enzymes is believed to delay senescence and quality deterioration in different kinds of fruit (Mirshekari, Madani, Yahia, Golding, & Vand, 2020; Jiang et al., 2021). Xu (Xu et al., 2021) proved that increased *SOD, CAT, POD* and their associated genes in pitaya during storage could efficiently lower the level of ROS and mitigate oxidative damage, development of decay and senescence. On the other hand, fungi can suppress antioxidant-induced pathways, such as hormone signal transduction pathways and enzymatic systems, which accelerate the impairment of host cells (Choudhary, Kumar, & Kaur, 2019). However, it has also been suggested that low concentrations of ROS play a central role in host defense by transmitting stimulatory signals to neighboring cells and activating host defense responses under both biotic and abiotic conditions (Mor et al., 2014). This might explain why MDA content of pitaya pulp in our study was suppressed after *A. flavus* contaminated pitaya cuticle, despite its cuticle senescence and rotting symptoms had been noticed, we speculated that in our study, exogenous Fe^{2+} could produce low dose of ROS and transmit stress signal on the fruit cuticle to inner cells.

It is commonly accepted that Fe^{2+} induced an ROS burst, accelerated cell membrane lipid peroxidation and accumulated MDA by ferroptosis, but our study proved that exogenous Fe^{2+} protected pitaya fruit from infection by postharvest pathogen *A. flavus* in a novel but potentially universal and easily applied way, which was different from classical ferroptosis, by directly inducing pathogen DNA breakdown. We found that Fe^{2+} might induce DNA breakage and upregulate DNA damage repair-related genes by directly binding to DNA and changing the DNA conformation, thus affecting its nature and blocking SOS repair pathways in *A. flavus* (Fig. 5**A-C**). It has been proven in some studies that metal ions are inextricably involved in nucleic acids due to their polyanionic nature and are responsible for large conformational changes. Additionally, the dynamic nature of nucleic acids is reflected in the characteristics of interactions with metal ions (Pechlaner & Sigel, 2012). In particular, the importance of Fe^{2+} binding to DNA has been considered in relation to DNA damage and mutations. (Loeb et al., 1988). It is assumed that there might exist some interactions between Fe^{2+} and

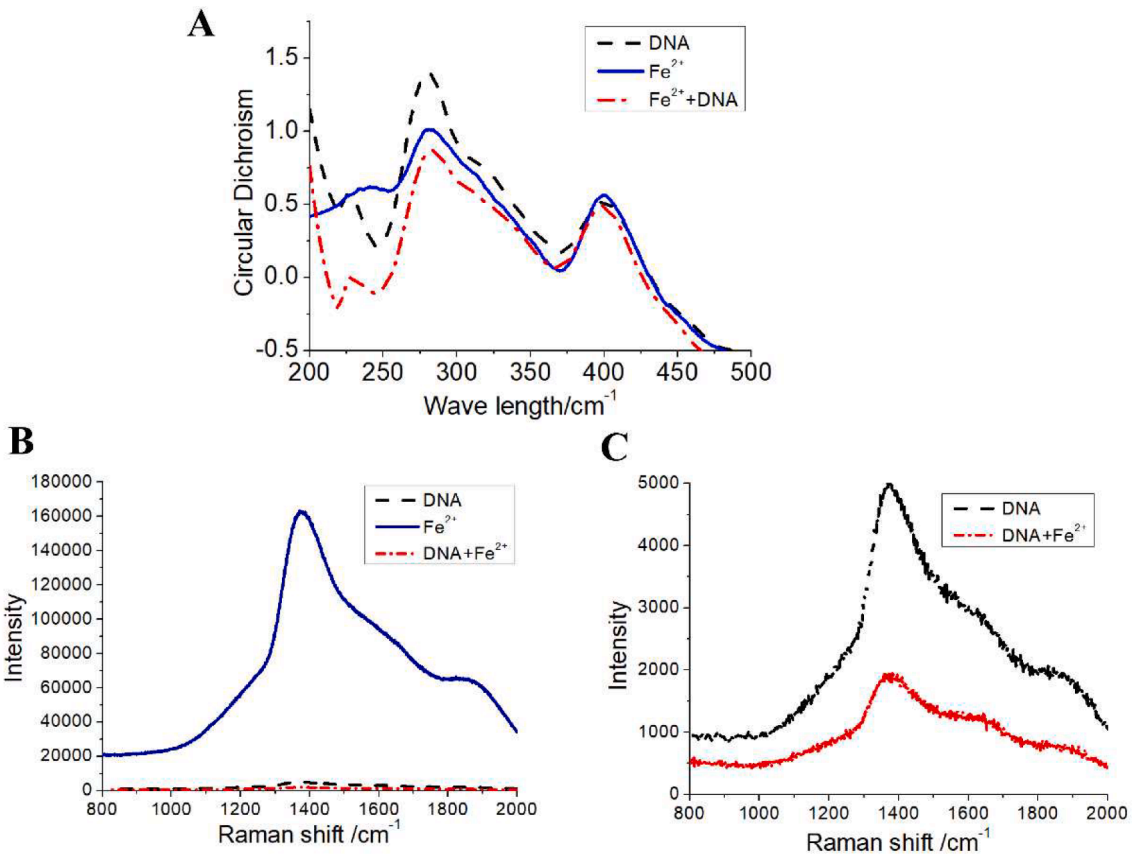

Fig. 6. CD spectroscopy and Raman spectra analysis of DNA upon binding to Fe ion solution.

DNA, and although some studies using calf thymine DNA as materials have shown that Fe^{2+} might bind to the backbone phosphate group and affect cleavage in DNA (Ouameur, Arakawa, Ahmad, Naoui, & Tajmir-Riahi, 2005), few studies have focused on the direct affinity of Fe^{2+} and DNA under physiological conditions. In this study, we performed agar electrophoresis analysis, the results showed that the levels of DNA fade with increasing concentrations of Fe^{2+}, and similar results were observed in the PCR products and in the process of PCR (Fig. 5**D-F**). Circular dichroism (CD) (Fig. 6**A**) and Raman (Fig. 6**B-C**) experiments were even more intuitive in that there was an interaction between Fe^{2+} and DNA, exogenous even low concentration of Fe^{2+} could change DNA conformation. As a result, the SOS response in A. *flavus* might be initiated because the SOS response is believed to be the mode of the survival strategy and allows microorganisms to evolve from an unfavorable environment (Keseler et al., 2013).

Recently, an increasing number of studies have reported that several nontoxic inorganic compounds, such as Ca^{2+}, Zn^{2+}, Cu^{2+} and Ni^{2+}, have been effectively utilized as additives in postharvest food to maintain flesh and extend shelf life of many fruit (Milosevic et al., 2017; Ahankari, Subhedar, Bhadauria, & Dufresne, 2021; Meena et al., 2020). For example, Ca^{2+} treatment could alleviate fruit postharvest chilling damage by protecting membrane structure and reducing cell wall breakdown, thus reducing the chance of pathogen infection (Manganaris, Vasilakakis, Diamantidis, & Mignani, 2010; Gupta, Jawandha, & Gill, 2011). It has been reported in some studies that pretreatment with Ca^{2+} reduced the occurrence of anthracnose and brown rot severity of pitaya fruit (Ghani, Awang, & Sijam, 2011). In addition to protecting the membrane, it has also been suggested that Ca^{2+}, as an intracellular second messenger, can transmit stress signals and activate various physiological responses in cells (Hepler, 2005). Sardella proved that Zn^{2+} had antifungal efficiency against several fungal contaminants (Sardella, Gatt, & Valdramidis, 2017). ZnO micro- and nanoparticle-based edible coatings have been successfully regarded as antibacterial agents and exhibit remarkable efficiency in extending shelf life of fruit, which is attributed to their ability to promote the production of reactive radicals. (La, Nguyen-Tri, Le, Nguyen, & Nguyen, 2021; Khla et al., 2021). Cu^{2+} combined chitosan nanoparticles show the ability to extend shelf life of stored tomato (Meena et al., 2020), and Tsvetkov et al. showed that Cu^{2+}-dependent death occurred by means of direct binding to lipoylated components of the tricarboxylic acid (TCA) cycle (Tsvetkov et al., 2022).

These studies raise the potential application of metal iron in post-harvest food, and they are superior in their durability, low toxicity and ability to withstand severe conditions, such as high temperature and high pressure. The antifungal effect triggered by Fe^{2+} found in this study would be a more efficient strategy to prevent postharvest decay because it can kill pathogens at nucleic acid level, and Fe^{2+} might be a universal antifungal agent against other postharvest pathogens. Combining Fe^{2+} and other postharvest protection methods will be a higher priority to prevent fruit postharvest fungal contamination to extend fruit shelf life.

5. Conclusion

In this study, we demonstrated that exogenous low dose within safe limit (3 mM) of Fe^{2+} could defend *A. flavus* infection and extend shelf life of postharvest pitaya fruit, by suppressing weight loss, constraining fruit decay, retaining fruit firmness, reducing titratable acid content and retaining total betalain content both during preservation and during infection with *A. flavus*. Antioxidant-related substances, including total phenols, *CAT, SOD* and *POD,* were enhanced after Fe^{2+} treatment. Moreover, these beneficial effects of Fe^{2+} might be achieved by two aspects. One was activating the antipathogen-related pathway inside the fruit by transmitting the stress response signal from the pericarp after *A. flavus* infection. On the other hand, Fe^{2+} could control colonization of

A. flavus by means of directly binding to *A. flavus* DNA and affecting the conformation of DNA, eventually leading to DNA breakage. Furthermore, transcription analysis revealed that Fe^{2+} could elicit DNA damage repair-related genes.

This is the first report about Fe^{2+} directly binding to fungal DNA, resulting in DNA breakage to eliminate fungi, and the study raises the possibility of Fe^{2+} application as a safer, less expensive and more eco-friendly antifungal agent.

CRediT authorship contribution statement

Lishan Yao: Project administration, Conceptualization, Writing – original draft, Methodology. **Tao Zhang:** Project administration, Methodology. **Shurui Peng:** Writing – review & editing. **Dan Xu:** Writing – review & editing. **Zhenbin Liu:** Writing – review & editing. **Hongbo Li:** Writing – review & editing. **Liangbin Hu:** Funding acquisition, Supervision, Writing – review & editing. **Haizhen Mo:** Writing – review & editing.

Declaration of Competing Interest

The authors declare that they have no known competing financial interests or personal relationships that could have appeared to influence the work reported in this paper.

Acknowledgments

This work was supported by the National Natural Science Foundation of China (Grant Nos. 31901795 and 32172321), the National Key Research and Development Program of China (Grant No. 2019YFC1606302) and the China Postdoctoral Science Foundation (2021M702057).

Appendix A. Supplementary data

Supplementary data to this article can be found online at https://doi.org/10.1016/j.fochms.2022.100135.

References

Ahankari, S. S., Subhedar, A. R., Bhadauria, S. S., & Dufresne, A. (2021). Nanocellulose in food packaging: A review. *Carbohydrate Polymers, 255*, Article 117479. https://doi.org/10.1016/j.carbpol.2020.117479

Ba, L. J., Cao, S., Ning, J. I., Chao, M. A., & Luo, D. (2022). Exogenous melatonin treatment in the postharvest storage of pitaya fruits delays senescence and regulates reactive oxygen species metabolism. *Food Science and Technology, 42*(5). https://doi.org/10.1590/fst.15221

Bordoh, P. K., Ali, A., Dickinson, M., Siddiqui, Y., & Romanazzi, G. (2019). A review on the management of postharvest anthracnose in dragon fruits caused by *Colletotrichum spp*. *Crop Protection, 130*, Article 105067. https://doi.org/10.1016/j.cropro.2019.105067

Choudhary, A., Kumar, A., & Kaur, N. (2019). ROS and oxidative burst: Roots in plant development. *Plant Diversity, 42*(1), 33–43. https://doi.org/10.1016/j.pld.2019.10.002

Christmann, M., & Kaina, B. (2013). Transcriptional regulation of human DNA repair genes following genotoxic stress: Trigger mechanisms, inducible responses and genotoxic adaptation. *Nucleic Acids Research, 41*(18), 8403–8420. https://doi.org/10.1093/nar/gkt635

Fiore, M., Cascella, M., Bimonte, S., Maraolo, A. E., Gentile, I., & Schiavone, V. (2018). Liver fungal infections: An overview of the etiology and epidemiology in patients affected or not affected by oncohematologic malignancies. *Infection and Drug Resistance, 29*(11), 177–186. https://doi.org/10.2147/IDR.S152473

Ghani, M., Awang, Y., & Sijam, K. (2011). Disease occurrence and fruit quality of pre-harvest calcium treated red flesh dragon fruit (*Hylocereus polyrhizus*). *African. Journal of Biotechnology, 10*, 1550–1558. https://doi.org/10.5897/AJB10.1440

Guo, Y., Breeden, L. L., Zarbl, H., Preston, B. D., & Eaton, D. L. (2005). Expression of a human cytochrome p450 in yeast permits analysis of pathways for response to and repair of aflatoxin-induced DNA damage. *Molecular and Cellular Biology, 25*(14), 5823–5833. https://doi.org/10.1128/MCB.25.14.5823-5833.2005

Gupta, N., Jawandha, S. K., & Gill, P. S. (2011). Effect of calcium on cold storage and poststorage quality of peach. *Journal of. Food Science and Technology, 48*, 225–229. https://doi.org/10.1007/s13197-010-0116-z

Harvey, T., Zkik, A., Auges, M., & Clavel, T. (2016). Assessment of iron deficiency and anemia in pregnant women: An observational French study. *Womens Health, 12*(1), 95–102. https://doi.org/10.2217/whe.15.91

Hepler, P. K. (2005). Calcium: A central regulator of plant growth and development. *The Plant Cell, 17*(8), 2142–2155. https://doi.org/10.1105/tpc.105.032508

Jiang, M., Pang, X., Liu, H., Lin, F., Lu, F., Bie, X., et al. (2021). Iturin A induces resistance and improves the quality and safety of harvested cherry tomato. *Molecules, 26*(22), 6905. https://doi.org/10.3390/molecules26226905

Jiang, Y. L., Chen, L. Y., Lee, T. C., & Chang, P. T. (2020). Improving postharvest storage of fresh red-fleshed pitaya (*Hylocereus polyrhizus sp.*) fruit by pre-harvest application of CPPU. *Scientia Horticulturae, 273*(1), Article 109646. https://doi.org/10.1016/j.scienta.2020.109646

Jomova, K., & Valko, M. (2011). Advances in metal-induced oxidative stress and human disease. *Toxicology, 283*(2–3), 65–87. https://doi.org/10.1016/j.tox.2011.03.001

Keseler, I. M., Mackie, A., Peralta-Gil, M., Santos-Zavaleta, A., Gama-Castro, S., Bonavides-Martínez, C., et al. (2013). EcoCyc: Fusing model organism databases with systems biology. *Nucleic Acids Research, 41*, D605–D612. https://doi.org/10.1093/nar/gks1027

Khla, B., Dbn, C., Ldta, B., Hong, P., Cvt, E., Kvt, E., et al. (2021). A novel antimicrobial Zno nanoparticles-added polysaccharide edible coating for the preservation of postharvest avocado under ambient conditions. *Progress in Organic Coatings, 158*, Article 106339. https://doi.org/10.1016/j.porgcoat.2021.106339

Kumar, V., Mishra, R. K., Kaur, G., & Dutta, D. (2017). Cobalt and nickel impair DNA metabolism by the oxidative stress independent pathway. *Metallomics, 9*(11), 1596–1609. https://doi.org/10.1039/c7mt00231a

La, D. D., Nguyen-Tri, P., Le, K. H., Nguyen, P. & Nguyen, D. D. (2021). Effects of antibacterial zno nanoparticles on the performance of a chitosan/gum arabic edible coating for post-harvest banana preservation. *Progress in Organic Coatings*, 151, 106057. https:doi.org/10.1016/j.porgcoat.2020.106057.

Lin, Y., Chen, M., Lin, H., Hung, Y. C., Lin, Y., Chen, Y., et al. (2017). DNP and ATP induced alteration in disease development of Phomopsis longanae Chi-inoculated longan fruit by acting on energy status and reactive oxygen species production-scavenging system. *Food Chemistry, 228*, 497–505. https://doi.org/10.1016/j.foodchem.2017.02.045

Loeb, L. A., James, E. A., Waltersdorph, A. M., & Klebanoff, S. J. (1988). Mutagenesis by the autoxidation of iron with isolated DNA. *Proceedings of the National Academy of Sciences of the United States of America, 85*(11), 3918–3922. https://doi.org/10.1073/pnas.85.11.3918

Manganaris, G. A., Vasilakakis, M., Diamantidis, G., & Mignani, I. (2010). Effect of in-season calcium applications on cell wall physicochemical properties of nectarine fruit (*Prunus persica* var. *Nectarina ait*. Maxim) after harvest or cold storage. *Journal of the Science of Food and Agriculture, 86*, 2597–2602. https://doi.org/10.1002/jsfa.2654

Meena, M., Pilania, S., Pal, A., Mandhania, S., Bhushan, B., Kumar, S., et al. (2020). Cu-chitosan nano-net improves keeping quality of tomato by modulating physio-biochemical responses. *Scientific Reports, 10*(1), 21914. https://doi.org/10.1038/s41598-020-78924-9

Milosevic, I., Jayaprakash, A., Greenwood, B., Driel, B., Rtimi, S., & Bowen, P. (2017). Synergistic effect of fluorinated and N Doped TiO_2 nanoparticles leading to different microstructure and enhanced photocatalytic bacterial inactivation. *Nanomaterials, 7*(11), 391. https://doi.org/10.3390/nano7110391

Mirshekari, A., Madani, B., Yahia, E. M., Golding, J. B., & Vand, S. H. (2020). Postharvest melatonin treatment reduces chilling injury in sapota fruit. *Journal of the Science of Food and Agriculture, 100*(5), 1897–1903. https://doi.org/10.1002/jsfa.10198

Mor, A., Koh, E., Weiner, L., Rosenwasser, S., Sibony-Benyamini, H., & Fluhr, R. (2014). Singlet oxygen signatures are detected independent of light or chloroplasts in response to multiple stresses. *Plant Physiology, 165*(1), 249–261. https://doi.org/10.1104/pp.114.236380

Ong, Y. Y., Wen, S. T., Mohamad, R., Sieo, C. C., & Tey, B. T. (2014). Biochemical and molecular identification of enterococcus spp. from red pitaya. *Process Biochemistry, 49*(4), 563–568. https://doi.org/10.1016/j.procbio.2014.01.019

Ouameur, A. A., Arakawa, H., Ahmad, R., Naoui, M., & Tajmir-Riahi, H. A. (2005). A Comparative study of Fe(II) and Fe(III) interactions with DNA duplex: Major and minor grooves bindings. *DNA and Cell Biology, 24*(6), 394–401. https://doi.org/10.1089/dna.2005.24.394

Pace, B., & Cefola, M. (2021). Innovative preservation technology for the fresh fruit and vegetables. *Foods, 10*(4), 719. https://doi.org/10.3390/foods10040719

Pechlaner, M., & Sigel, R. K. (2012). Characterization of metal ion-nucleic acid interactions in solution. *Metal Ions in Life Sciences, 10*, 1–42. https://doi.org/10.1007/978-94-007-2172-2_1

Punihaole, D., Workman, R. J., Upadhyay, S., Van Bruggen, C., Schmitz, A. J., Reineke, T. M., et al. (2018). New Insights into Quinine-DNA Binding Using Raman Spectroscopy and Molecular Dynamics Simulations. *The Journal of Physical Chemistry B, 122*(43), 9840–9851. https://doi.org/10.1021/acs.jpcb.8b05795

Sardella, D., Gatt, R., & Valdramidis, V. P. (2017). Physiological effects and mode of action of ZnO nanoparticles against postharvest fungal contaminants. *Food Research International, 101*, 274–279. https://doi.org/10.1016/j.foodres.2017.08.019

Shen, Q., Liang, M., Yang, F., Deng, Y. Z., & Naqvi, N. I. (2020). Ferroptosis contributes to developmental cell death in rice blast. *New Phytologist, 227*(6), 1831–1846. https://doi.org/10.1111/nph.16636

Tan, X. L., Zhao, Y. T., Shan, W., Kuang, J. F., Lu, W. J., Su, X. G., et al. (2020). Melatonin delays leaf senescence of postharvest Chinese flowering cabbage through ROS homeostasis. *Food Research International, 138*(Pt B), Article 109790. https://doi.org/10.1016/j.foodres.2020.109790

Toivonen, Peter M. A & Brummell David, A. (2008). Biochemical bases of appearance and texture changes in fresh-cut fruit and vegetables. *Postharvest Biology & Technology*, 48.1(2008), 1-14. https://doi.org/10.1016/j.postharvbio.2007.09.004.

Tsvetkov, P., Coy, S., Petrova, B., Dreishpoon, M., Verma, A., Abdusamad, M., et al. (2022). Copper induces cell death by targeting lipoylated TCA cycle proteins. *Science, 375*(6586), 1254–1261. https://doi.org/10.1126/science.abf0529

Umesha, S., Manukuma, R. H. M., Chandrasekhar, B., Shivakumara, P., Shiva, K. J., Raghava, S., et al. (2017). Aflatoxins and food pathogens: Impact of biologically active aflatoxins and their control strategies. *Journal of Science and Food Agriculture, 97*(6), 1698–1707. https://doi.org/10.1002/jsfa.8144

Xu, Y., Cai, Z., Ba, L., Qin, Y., Su, X., Luo, D., et al. (2021). Maintenance of postharvest quality and reactive oxygen species homeostasis of pitaya fruit by essential oil p-anisaldehyde treatment. *Foods, 10*(10), 2434. https://doi.org/10.3390/foods10102434

Yao, L., Ban, F., Peng, S., Xu, D., Li, H., Mo, H., et al. (2021). Exogenous iron induces NADPH oxidases-dependent ferroptosis in the conidia of *Aspergillus flavus*. *Journal of Agricultural and Food Chemistry*, 69(45), 13608-13617. https://doi.org/ 10.1021/acs.jafc.1c04411.

Zahid, N., Ali, A., Siddiqui, Y., & Maqbool, M. (2013). Efficacy of ethanolic extract of propolis in maintaining postharvest quality of dragon fruit during storage. *Postharvest Biology & Technology, 79*, 69–72. https://doi.org/10.1016/j.postharvbio.2013.01.003